Electric Field Effects on Indirect Optical Transitions in Silicon*†

P. H. WENDLAND
Hughes Research Laboratories, Malibu, California

AND

MARVIN CHESTER
University of California, Los Angeles, California

(Received 10 June 1965)

The effects of an externally applied electric field on the absorption of light by silicon have been measured under a wide variety of experimental conditions. The measurements on 52 samples of both n and p type and a variety of doping species show conclusively that the electro-absorption spectrum is associated with the pure silicon lattice and not with any impurity or imperfection. The spectral characteristics of the electro-absorption peaks associated with phonon-assisted processes are strongly affected by the magnitude of the applied electric field over the measured range of 10^4 to 10^6 V/cm. The electro-absorption spectrum is unchanged, however, in relative magnitude and peak position by a change in temperature, and the absolute spectral positions follow the band-gap dependence on temperature. Concurrent measurements of the maximum-electro-absorption-peak position and high-resolution, field-free optical absorption establish the final state in the transition process as an exciton state. An interpretation of these measurements is given, based on an optically assisted tunneling process to a final exciton state.

INTRODUCTION

A MEASURABLE change in the absorption edge of a semiconductor or insulator when a high electric field is applied was predicted theoretically by Franz[1] and independently by Keldysh.[2] A simple physical basis for this effect was given in Franz's work that could be called "optically assisted Zener tunneling." An electron at the top of the valence band moving under the influence of an applied electric field experiences a potential barrier to its transition to the lowest conduction-band state. The width of this barrier, as shown in Fig. 1, is inversely proportional to the magnitude of of the applied electric field E, and directly proportional to the forbidden band gap E_g. A typical Zener tunneling process would transfer an electron from the valence band through the barrier and into the conduction band. For materials with band gaps above 1 eV, the transition probability for this complete tunneling process is extremely small[3] for attainable values of applied electric fields. A greater probability obtains, however, for the electron to penetrate a short distance into the ordinarily forbidden region and temporarily occupy a state above the zero-field valence-band maxima. The absorption of a photon from this higher energy state gives rise to an increased absorption coefficient on the low-photon-energy side of the zero-field absorption edge. Callaway[4] has developed a complete quantum-mechanical treatment of this electric-field effect on direct optical transitions, and he finds an increase in long-wavelength edge absorption as well as several types of "oscillations" of the electric-field-induced differential absorption coefficient. Penchina,[5] and Chester and Fritsche[6] have recently worked out the theory of the effect of an electric field on indirect, phonon-assisted transitions. They find effects which are qualitatively similar but different in form and magnitude from those for direct transitions, and displaced from the band gap energy by the energy of the participating phonon.

Several investigators have found the predicted change in the optical-absorption edge in a variety of materials exhibiting direct transitions.[7–9] Quantitative agreement between theory and experiment has been obtained in a number of recent experiments.[10]

We have observed the effects of an electric field on optical-absorption processes in silicon throughout the

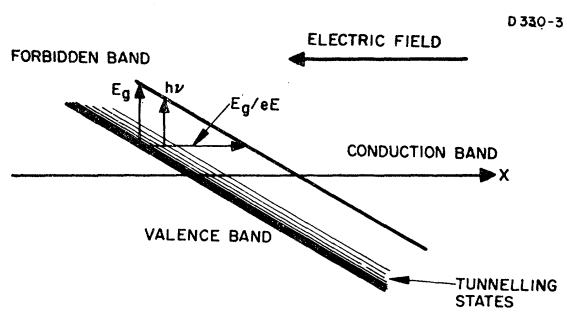

FIG. 1. Real-space energy-level diagram with electric field.

* This paper is part of a thesis submitted to the graduate division of the University of California at Los Angeles in partial fulfillment of the requirements for the Ph.D. degree. The work was performed while the author was concurrently associated with Hughes Research Laboratories.

† This work was supported in part by the U. S. Atomic Energy Commission.

[1] W. Franz, Z. Naturforsch. **13**, 484 (1958).

[2] L. V. Keldysh, Zh. Eksperim. i Teor. Fiz. **34**, 1138 (1958) [English transl.: Soviet Phys.—JETP **7**, 788 (1958)].

[3] C. Zener, Proc. Roy. Soc. (London) **145**, 523 (1934).

[4] J. Callaway, Phys. Rev. **130**, 549 (1963).

[5] C. Phenchina, Phys. Rev. **138**, A924 (1965).

[6] M. Chester and L. Fritsche, Phys. Rev. **139**, A518 (1965).

[7] R. Williams, Phys. Rev. **126**, 442 (1962).

[8] T. S. Moss, J. Appl. Phys. **32**, 2136 (1962).

[9] V. S. Vavilov and K. I. Britsyn, Fiz. Tverd. Tela **2**, 1937 (1960) (English transl.: Soviet Phys.—Solid State **2**, 1746 (1961)].

[10] A. Frova and P. Handler, Phys. Rev. **137**, A1857 (1965).

region of phonon-assisted indirect transitions.[11,12] Here, the effects of phonon participation introduce peaks and valleys in the electric-field-induced differential absorption coefficient. It has been determined by Handler and Frova[13] that phonon-energy assignments can be made directly from the photon energy separation between electro-absorption peaks. It is the purpose of this paper to present data on these electro-absorption peaks taken in over 50 silicon samples of varying purity and with a complete range of experimental conditions: electric-field strengths from 10^4 to 10^6 V/cm, temperatures from 300 to 77°K, and three crystallographic orientations. A theoretical interpretation of this data is given based on an "optically assisted tunneling process" to final exciton states.

EXPERIMENTAL

The experimental equipment that was used to obtain these measurements was essentially the same as that described in our earlier work.[11,12] Steady unchopped light from a grating monochromator was focused on the Si sample located a few mm away from the exit slit. Square-wave voltage pulses were applied to the sample with a frequency of 50 cps and a duty cycle of 10%. The field variations produced by these pulses changed the absorption coefficient of the specimen. The light transmitted by the Si was detected with a PbS cell located a few millimeters behing the Si. The detector output voltage varied with the change in transmitted intensity produced by the 50-cps field variations. This output was fed to an ac pre-amplifier and then to a lock-in amplifier which was synchronized to the 50-cps voltage pulses. Readings were taken from the meter on the lock-in amplifier and also from a recorder attached to the output. An oscilloscope monitored the amplified detector-output waveform for viewing under high-signal conditions.

The equipment that was used for obtaining the electroabsorption spectrum as a function of temperature is shown in Fig. 2. The incident light is applied to the sample at the bottom of the Dewar through a light guide and detected with a PbS cell located directly below the sample. A range of temperatures between 4 and 300°K was obtained by varying the distance between the liquid-nitrogen or helium level in the inner Dewar and the copper block containing the Si sample and detector.

The 52 specimens used were made from both p and n type silicon wafers with resistivities in different samples ranging from 1 to 10 000 Ωcm. pn junctions were formed on the Si wafers in order to obtain high electric fields with low current flow under an applied reverse-bias voltage. A shallow phosphorus diffused junction was used on p-type wafers and a surface-barrier junction on n-type wafers.[14] An evaporated transparent aluminum film was used as a back electrode for both n and p wafers. The thickness of different completed samples ranged from 50 to 300 μ. The junction areas varied from 0.5 to 1 cm². The light was applied perpendicularly to the junction surface and traversed the junction, the sample thickness, and the back electrode before entering the PbS detector.

The differential absorption coefficient due to the applied electric field is obtained from the relationship

$$\Delta\alpha = (\Delta T/T)W(E), \tag{1}$$

where $\Delta\alpha$ = absorption coefficient with electric field minus absorption coefficient without field, ΔT = differential transmission signal, T is the total transmission in zero field, and W is the distance over which the applied field E is maintained. ΔT and T are the quantities actually measured in the optical setup, and E and W are obtained as a function of applied reverse bias voltage through capacitance measurements. The combination of these measured quantities through Eq. (1) gives the differential absorption coefficient as a function of applied electric field.

Equation (1) should, in principle, contain a multiplicative factor involving the reflectivities of the various surfaces involved. However, except for the values recorded in Fig. 3, the absolute magnitude of $\Delta\alpha$ has no bearing on what follows. The values indicated in the figure may, in fact, be somewhat too large. They are offered, however, merely to indicate the approximate magnitude of the effect.

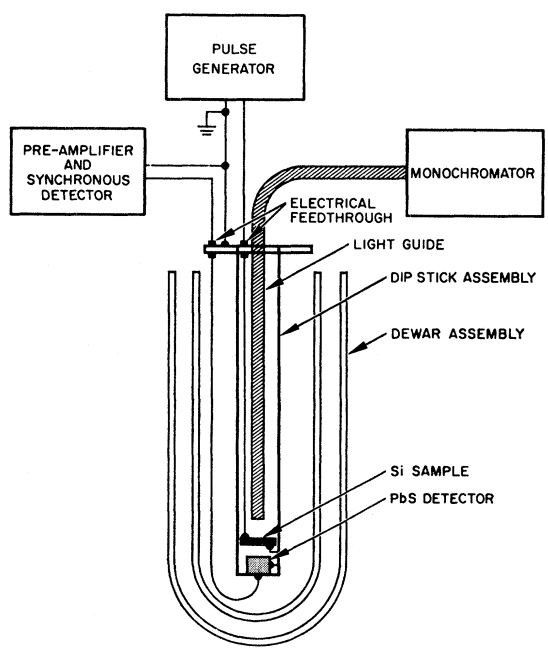

FIG. 2. Low-temperature measurement system.

[11] M. Chester and P. Wendland, Phys. Rev. Letters **13**, 193 (1964).
[12] P. Wendland, Bull. Am. Phys. Soc. **9**, 552 (1964).
[13] A. Frova and P. Handler, Phys. Rev. Letters **14**, 178 (1965).
[14] J. M. Taylor, *Semiconductor Particle Detectors* (Butterworths Scientific Publications Inc., Washington, 1963).

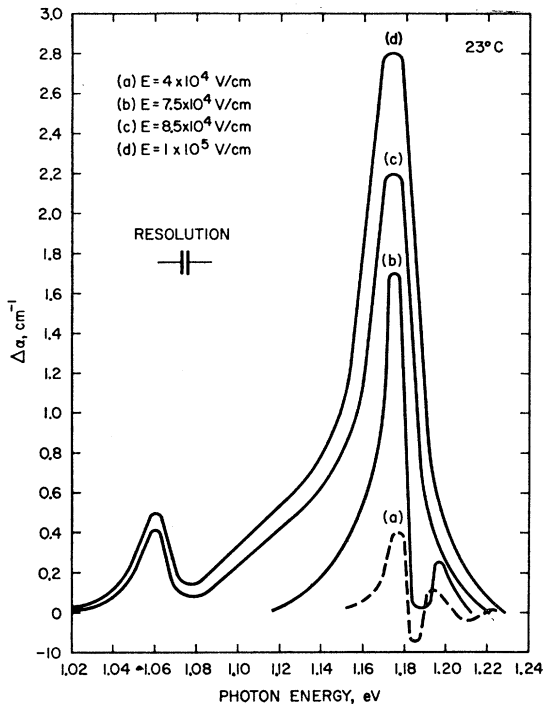

FIG. 3. Electro-absorption spectrum of silicon.

MEASUREMENTS

The compilation of electro-absorption data from a large number of silicon samples of both n and p type is given in Fig. 3. The sample types from which this data was obtained are given in Table I. A number of samples from each of the listings of Table I were used for a total of 52 tested samples. A complete range of field strengths could not be obtained in every sample, since low-resistivity material builds up very high electric fields over short depletion depths with relatively low applied voltages, while high-resistivity material depletes to such large distances that electric fields of 10^6 V/cm are unattainable before applied voltage induced surface breakdown is initiated. However, large regions of attainable electric fields overlapped from sample to sample. Additionally, the high-resistivity fully depleted p-i-n structures allowed measurements to be taken in electric fields that were uniform across the sample thickness.

TABLE I. Silicon crystals used in electro-absorption studies.

Type	Resistivity	Impurity concentration	Major impurity type	Major electroabsorption peak position
p	10,000 Ω cm	1.4×10^{12}/cm³	trace only	1.175 eV, 1.06 eV
p	500 Ω cm	2.8×10^{13}/cm³	boron	1.175 eV, 1.06 eV
p	60 Ω cm	2.3×10^{14}/cm³	boron	1.175 eV, 1.06 eV
p	1.5 Ω cm	0.93×10^{16}/cm²	aluminum	1.175 eV, 1.06 eV not obtainable
n	2000 Ω cm	2.6×10^{12}/cm³	trace only	1.175 eV, 1.06 eV
n	270 Ω cm	2.0×10^{13}/cm³	phosphorus	1.175 eV, 1.06 eV
n	55 Ω cm	0.95×10^{14}/cm³	phosphorus	1.175 eV, 1.06 eV
n	6 Ω cm	0.87×10^{15}/cm³	antimony	1.175 eV, 1.06 eV not obtainable

Two main electro-absorption regions are observed in Fig. 3. The region around 1.175 eV and the region around 1.059 eV. From the optical absorption data of MacFarlane *et al.*,[15] it would be inferred that the structure at 1.175 eV is associated with phonon emission processes, while the electro-absorption structure at 1.059 eV is associated with phonon absorption processes. In order to check this assumption, electro-absorption data as a function of temperature was obtained. Figure 4 shows the variation of the magnitude of the two main electro-absorption peaks as the temperature is varied. The peak at 1.175 eV, associated with phonon emission, remains constant with temperature, while the peak at 1.059 eV, associated with phonon absorption, decreases rapidly as the temperature is lowered, thus verifying the phonon emission and absorption assignments. The variation with temperature of the three main electro-absorption peaks associated with phonon emission, at a constant field strength of 2×10^4 V/cm, is given in Fig. 5. Also plotted in Fig. 5 is MacFarlane's data[15] for the onset of the emission of 670°K phonons, as given in his Table I. It is observed that the spectral positions of the electro-absorption peaks maintain a constant energy separation between themselves and the energy position of the onset of the 670°K-phonon emission, as the temperature is varied. The spectral variation of electro-absorption peak positions with temperature can thus be attributed entirely to the change

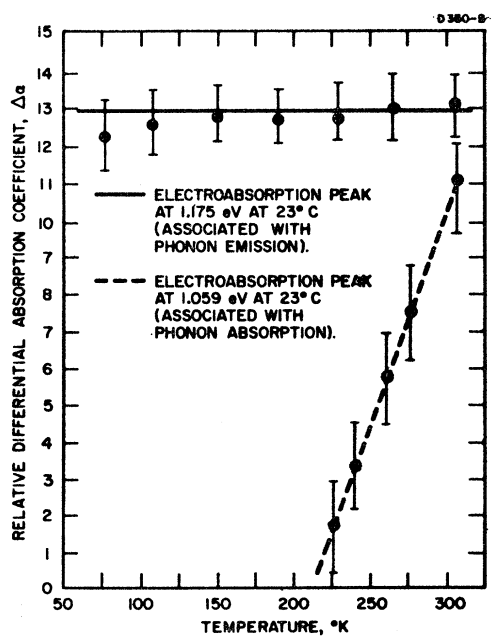

FIG. 4. Electro-absorption-peak-magnitude variation with temperature

[15] G. G. MacFarlane, T. P. McLean, J. E. Quarrington, and V. Roberts, Phys. Rev. 111, 1245 (1958).

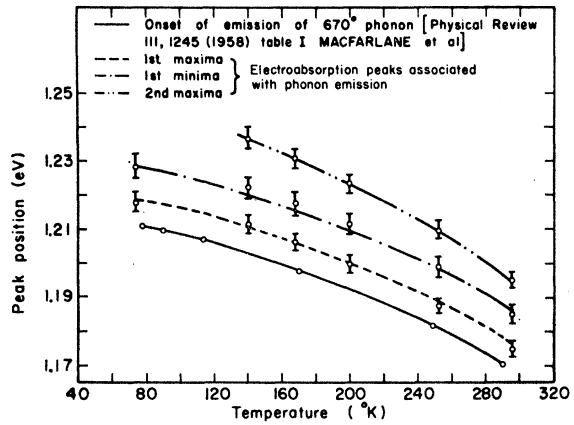

FIG. 5. Spectral variation of electro-absorption peaks with temperature.

of the bandgap energy with temperature. Electro-absorption structure is thus associated with the bandgap energy in an analogous fashion to electric-field-free optical absorption.

It is observed in Fig. 3 that as the electric field strength is raised from 2×10^4 to 8×10^4 V/cm, the "oscillatory" behavior of the differential absorption coefficient is replaced by one smooth positive peak. During this process, the spectral-energy position of the main positive peak at 1.175 eV does not vary, but does increase its half-width. The spectral-energy positions of the subsidiary peaks at 1.198 and 1.215 eV, vary only slightly with increasing electric-field strength, as they are taken over by the main positive peak. This behavior is consistent with our view, discussed in the following section, that the electro-absorption spectra is associated with exciton final states, since it is just in the electric-field-strength region discussed above that field ionization of exciton states in silicon is expected. The removal of much of the low-electric-field structure as the field increases can thus be associated with an electric-field-induced change in the distribution of exciton energy states.

Detail on the electro-absorption peak at 1.059 eV, associated with phonon emission, is given in Fig. 6. A detailed curve of our low-field electro-absorption data in the phonon emission region is presented in Fig. 7. This curve is similar to Fig. 1 of our first paper,[11] except for the resolving of an additional positive peak at 1.215 eV. The broad positive peak observed in earlier work[13] at about 1.27 eV has been found by us to have a relatively long time constant associated with it, rather than the detection system limited time constant of the electro-absorption signals. For this reason, we associate this peak with a thermally induced change of the absorption edge and have not included it in our electro-absorption data.

The effect of crystal orientation on the electro-absorption spectrum was early considered to be particularly significant in distinguishing between possible theoretical models, and measurements were obtained of the electro-absorption spectrum for three different orientations of the crystallographic axis relative to the light beam direction. Ten-mil-thick wafers were cut from a single ingot with surfaces in each of the three typical crystallographic planes: 111, 110, and 100. These sliced and lapped wafers were provided in both n and p type by Monosilicon Corporation. Junction samples were prepared using the techniques described previously. The measurement setup was the same as described previously with the light-beam direction parallel to the electric-field direction, and both perpendicular to the plane surface of the silicon wafer. The preparation of three samples, one in each orientation, of each type, n and p, was done simultaneously, so that no changes from sample to sample in the relative magnitude of the electro-absorption spectrum could be attributed to differences in processing. The results of electro-absorption measurements on n-type samples of different crystallographic orientation are given in Fig. 8, where a plot of electric-field-induced differential transmission as a function of incident photon energy is given. The data on p-type material is identical. There is no difference in the energy positions of maximum and minima differential transmission signals among the samples of differing orientation. There is a slight difference in the absolute magnitudes of the electric-field-induced differential transmission signals among the samples of different orientation. However, this difference can be accounted for on the basis of slightly differing electric-field strengths, as determined through measurements of barrier capacitance. These differences of electric-field

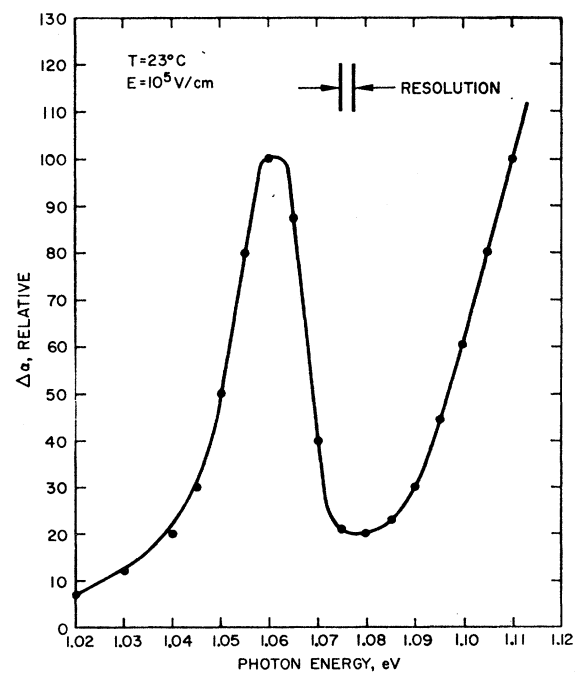

FIG. 6. Electro-absorption spectrum at 1.06 eV.

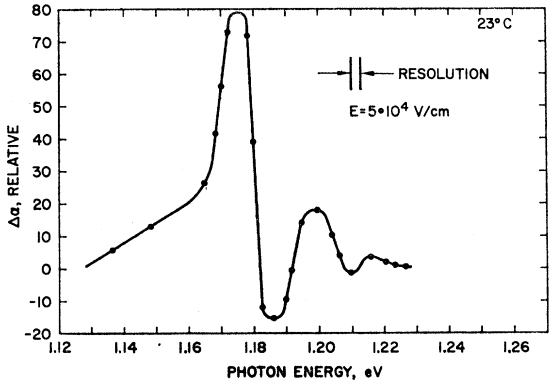

FIG. 7. Electro-absorption spectrum of silicon in the phonon-emission region at 5×10^4 V/cm.

strength arise naturally through slightly differing resistivities of the base material. After dividing the relative magnitude of the differential transmission signal by the capacitively determined electric field to normalize each curve of Fig. 8, the absolute magnitudes of the electric-field-induced differential transmission signals were found to be equal within 5% in the three different crystallographic directions tested.

In order to determine the spectral energy position of our electro-absorption peaks in relation to the exciton fine structure of MacFarlane *et al.*,[15] we obtained zero-field optical-absorption data in the same experimental setup as that used for electro-absorption data. A light-chopping wheel was used for straight optical-absorption measurements with electric field off, while the same optical system and electrical detection equipment were used for the electro-absorption measurements but without the chopping wheel. In the latter case, the electric field was pulsed at the same rate as that used for the chopping wheel in the former case. Using the same optics and electronics for both measurements, any possible absolute spectral-energy differences between our electro-absorption peak positions and previous straight absorption data were eliminated. We were particularly interested in determining the spectral-energy position of our major high field electro-absorption peak in relation to the spectral position at which MacFarlane's absorption coefficient data[15] shows the sharply rising inflection region indicative of the onset of transitions to final exciton states with phonon emission.

Figure 9 shows a simultaneous plot of the main electro-absorption peak at 8×10^5 V/cm and our experimental data on the optical transmission of this sample. The exciton "inflection point" is clearly visible at 1.175 eV in the optical transmission. The peak of the electro-absorption signal is also located at exactly this spectral energy position. The spectral energy position of the onset of transitions involving exciton states is separated from the onset of free carrier states by 0.01 eV.[16] Since the resolution involved in these measurements was always better than 0.003 eV, a differentiation can be made between exciton final states and free-carrier final states on the basis of relative spectral energy positions. We observe that such a spectral energy position comparison in Fig. 9 gives evidence in favor of an electric field induced process to final exciton states.

DISCUSSION OF RESULTS

The physical mechanism for electro-absorption in silicon that emerges from the collection of data given in the measurements section is perhaps best described in terms of an energy–**k**-vector diagram for electrons in silicon. The simplified but relevant features, for our purposes, of this band structure are given in Fig. 10. The valence band maxima occurs at $\mathbf{k}=0$, while the conduction band minima in silicon occurs in the $\langle 100\rangle$ direction at a value of **k** approximately 0.8 that at the Brillouin zone boundary.[17] The exciton binding energy has been determined as 0.01 eV, with a continuum of levels existing between this energy and the free carrier states.[15,16] The solid lines, representing indirect optical transitions, essentially depict conservation of energy and momentum relationships between electron, photon, and phonon, to a final exciton state. An electron transition through phonon emission to a final exciton state

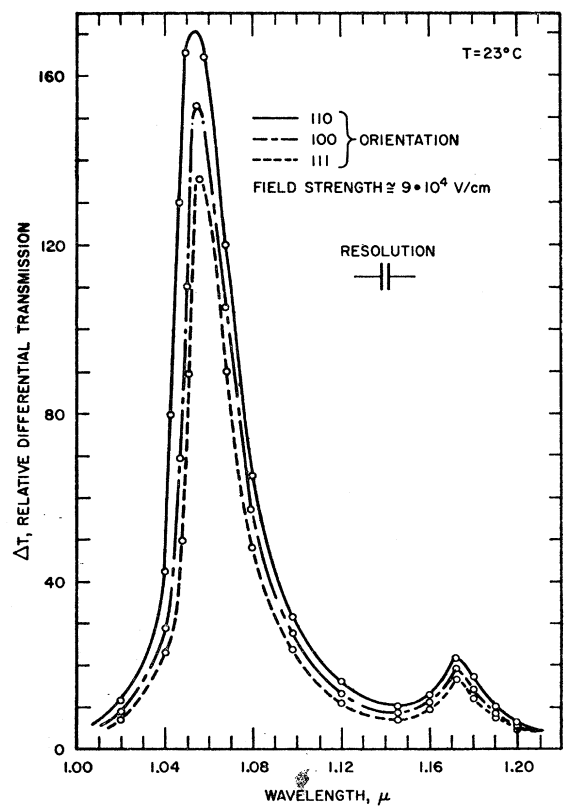

FIG. 8. Electro-absorption spectrum at differing crystallographic orientations.

[16] G. Dresselhaus, J. Phys. Chem. Solids **1**, 14 (1956).

[17] F. Herman, Proc. Inst. Radio Engrs. **43**, 1703 (1955).

produces a sharp rise in the optical absorption coefficient at a photon energy corresponding to the onset of this process, while a similar rise is observed in the phonon absorption process at a lower photon energy. The difference between the photon energies at which these two processes occur is just twice the value of the energy of the phonon involved. When a strong electric field is applied to the material, valence-band electrons can occupy states in the ordinarily forbidden region through the tunneling process that was depicted in Fig. 1. The occupation of higher lying forbidden-band energy states by what are ordinarily valence-band electrons under field excitation obviously leads to a general increase of low-energy absorption edge processes, plus a number of more subtle effects.[4–6] The most obvious experimental manifestation of this electric-field effect on transitions to final exciton states is then a relatively narrow spectral region of positive differential absorption coefficient. The question to be answered in silicon, and analogously germanium, is why this electric-field effect on optical transition is strongest for exciton final states, as determined experimentally, rather than free-carrier final states. Elliott[18] has shown that the onset of indirect transitions to exciton states is proportional to the one-half power of the energy while indirect transitions to free-carrier final states are proportional to the energy squared. Thus exciton transitions are manifested as inflection regions of steep slope when one plots the square root of the absorption coefficient of silicon

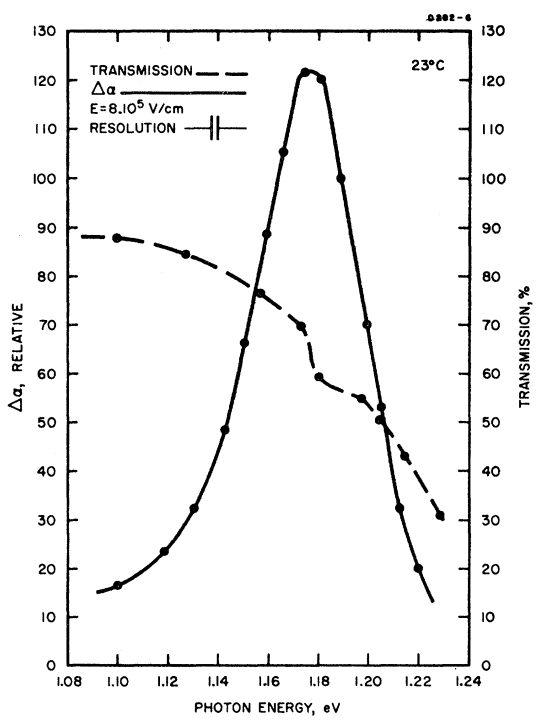

FIG. 9. Comparison of electro-absorption spectra with optical transmission.

[18] R. J. Elliot, Phys. Rev. **108**, 1384 (1957).

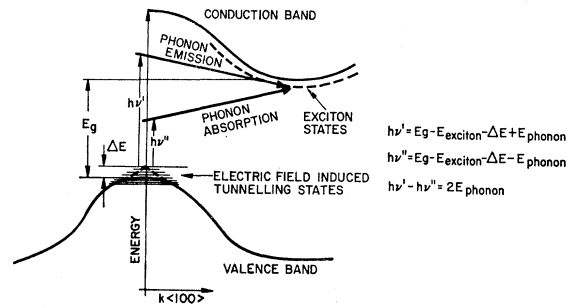

FIG. 10. Energy schematic for electroabsorption in silicon.

versus the photon energy.[15] Franz[1] has developed a phenomenological expression from his optically assisted tunneling theory which relates the electro-absorption signal to the slope of the field-free absorption coefficient. From his Eqs. (24) and (34),

$$\Delta\omega = \lambda^2 e^2 E^2 / 12hm, \tag{2}$$

where $\Delta\omega$ is the spectral energy change, λ is proportional to the slope of the field-free absorption coefficient, and E is the applied field. Electro-absorption signals thus provide a sensitive indicator of changes in slope in the zero-electric-field absorption coefficient. Since exciton transitions exhibit steep slopes in the zero-field absorption coefficient of Si over narrow spectral regions, they naturally give rise to large electric-field-induced absorption coefficient changes over the same relatively narrow spectral regions.

The two high peaks in Fig. 3, one at 1.175 eV and one at 1.055 eV, are then associated, respectively, with the "optically assisted tunneling" of phonon emission and phonon absorption processes to final exciton states depicted in Fig. 7. The spectral energy difference between these two electric-field-induced differential absorption coefficient peaks should thus give twice the energy of the phonon involved. From the high-electric-field data of Fig. 3, the phonon of major importance in the electro-absorption process in Si is one with an energy of (1.170 eV−1.059 eV)/2, or 58 meV. This phonon is known from neutron diffraction data[19] to be the transverse-optic (TO) phonon in silicon.

The low electric field electroabsorption data of this paper and previous work[11] show a more complex structure than the high field data, and consist of both positive and negative peaks. Frova and Handler[13] have shown that these peaks can be correlated with other single phonon energies than the TO, and combinations of phonons. The physical processes would remain the same, however, as that discussed above for the TO phonon. All of the theories to date for "optically assisted tunneling processes" show negative as well as positive peaks in the electric field induced differential absorption coefficient, and the negative peaks observed

[19] B. N. Brockhouse, Phys. Rev. Letters **2**, 256 (1959).
[20] D. Curie, *Luminescence in Crystals* (New York, John Wiley & Sons, Inc., 1963), p. 96.

experimentally are in accordance with such predictions.[4–6] It was shown in the measurements section that the plethora of structure in the electro-absorption spectrum at low electric fields was taken over by one broad positive peak as the field was raised above 5×10^4 V/cm. It was also shown that the final state in the transition process was an exciton state. We now wish to show that 5×10^4 V/cm is just the electric field strength which initiates field ionization of exciton states and thereby changes the energy distribution of these states. The binding energy of the exciton in Si has been determined to be 0.01 eV.[12,14] The radius of the first exciton Bohr orbit, a_0' in silicon is approximately $1\times6\times10^{-7}$ cm. The Stark effect for weakly bound excitons has been given as[20]

$$\Delta E=-\tfrac{3}{2}neEa_0', \tag{3}$$

for levels of principal quantum number n. Ionization of the level of principal quantum number 1 then onsets at an electric field strength of 5×10^4 V/cm. This is to be compared with the electric field strength range of 4×10^4–8×10^4 V/cm at which experimental results show a coalescence of structure into one broad positive electro-absorption peak.

PHYSICAL REVIEW VOLUME 140, NUMBER 4A 15 NOVEMBER 1965

Free-Carrier Magneto-Microwave Kerr Effect in Semiconductors*

M. E. Brodwin and R. J. Vernon†
Department of Electrical Engineering, Northwestern University, Evanston, Illinois
(Received 3 June 1965)

The free-carrier magneto-Kerr effect is analyzed in terms of R, the amplitude ratio of the two orthogonal linearly polarized components of the reflected wave, and δ, the phase difference between these two components. Equations relating R and δ to the elements of the magnetoconductivity tensor are presented for the plane-wave case and the TE_{11} mode in a circular waveguide. Simple approximate expressions for R and δ are given for the high-loss case where $\sigma_s/\omega\epsilon_s\gg1$, $\mu_H B\ll1$, and $\omega\tau\ll1$ (σ_s=zero-field dc conductivity; ϵ_s=static dielectric constant; μ_H=Hall mobility; τ=scattering time). These approximate expressions are compared with curves computed from the more complex expressions. The effect of multiple reflections within the semiconductor is considered. Experimental data for R and δ as functions of magnetic flux density and resistivity are presented for n-type germanium, n- and p-type silicon, and n-type indium antimonide at room temperature for the TE_{11} mode in a circular waveguide. It is found experimentally that the TE_{11}-mode analysis of the magneto-Kerr effect applies equally well to samples placed inside the circular waveguide and to those abutting on the end of the waveguide. Data on one n-type germanium and one n-type indium antimonide crystal are presented for temperatures between about 100 and 300°K. The effect of surface treatment on the measurements is also discussed.

I. INTRODUCTION

In recent years considerable attention has been given to the microwave Faraday effect in semiconductors.[1–6] It has been shown to be a powerful tool for the investigation of semiconductor transport parameters. However, since the Faraday effect depends upon transmission of electromagnetic radiation through the material, its measurement becomes difficult for the higher conductivity semiconductors where the energy transmitted through the sample is very small. In this high-conductivity range the magneto-Kerr effect, which occurs in the reflected wave, can often be measured. Because of its close relation to the Faraday effect, the magneto-Kerr effect can also be expected to yield valuable information concerning the semiconductor transport parameters.

The Kerr effect arises when a linearly polarized electromagnetic wave is incident upon the surface of a sample in the static magnetic field. The reflected wave is elliptically polarized with the major axis of the ellipse rotated with respect to the incident plane of polarization. Only the case of normal incidence with the magnetic field collinear with the direction of propagation is considered here. For this case, the origin of the ellipse can be explained qualitatively by considering the incident linearly polarized wave as being composed of two counter-rotating circularly polarized components. Since the lateral motions of the free-charge carriers in the static magnetic field are circular and in the same sense for all carriers of a given type, the two circularly polarized components react differently with the free-charge carriers. Thus, the two components have different reflection coefficients at the surface of the sample and,

* This work was supported by a National Defense Education Act Fellowship and the Advanced Research Projects Agency through the Northwestern University Materials Research Center.
† Present address: Electrical Engineering Department, University of Wisconsin, Madison, Wisconsin.
[1] R. Suhl and G. L. Pearson, Phys. Rev. **92**, 858 (1953).
[2] R. R. Rau and M. E. Caspari, Phys. Rev. **100**, 632 (1955).
[3] J. K. Furdyna and S. Broersma, Phys. Rev. **120**, 1995 (1960).
[4] J. K. Furdyna and M. E. Brodwin, Phys. Rev. **124**, 740 (1961).
[5] A. Bouwknegt and J. Volger, Physica **30**, 113 (1964).
[6] M. E. Brodwin and T. J. Burgess, Appl. Phys. Letters **5**, 223 (1964).